JACS
JOURNAL OF THE AMERICAN CHEMICAL SOCIETY

COMMUNICATION

pubs.acs.org/JACS

Semiconducting Organic Assemblies Prepared from Tetraphenylethylene Tetracarboxylic Acid and Bis(pyridine)s via Charge-Assisted Hydrogen Bonding

Pradeep P. Kapadia,[†] Lindsay R. Ditzler,[†] Jonas Baltrusaitis,[†,‡] Dale C. Swenson,[†] Alexei V. Tivanski,[†] and F. Christopher Pigge*[,†]

[†]Department of Chemistry and [‡]Central Microscopy Research Facility, University of Iowa, Iowa City, Iowa 52242, United States

Supporting Information

ABSTRACT: Principles of crystal engineering have been applied toward the construction of supramolecular assemblies between an acid-functionalized tetraphenylethylene derivative and three different bis(pyridine)s [4,4′-bis(pyridyl)-ethylene, 4,4′-bis(pyridyl)ethane, and 4,4′-bipyridine]. Each assembly was structurally characterized, and charge transfer interactions within each sample were visually apparent. Quantum chemical calculations were used to determine crystal band structure and band gap magnitude, and electrical properties of the materials were measured using conducting probe atomic force microscopy (CP-AFM). The crystals displayed charge-carrier capability, and the magnitude of semiconductivity varied systematically as a function of conjugation in the bis(pyridine) component. Crystals incorporating 4,4′-bis(pyridyl)ethylene and 4,4′-bipyridine displayed conductivities comparable to those of established organic semiconductors (μ_{eff} = 0.38 and 1.7 × 10^{-2} $cm^2/V\cdot s$, respectively).

Achieving the ability to control the form of supramolecular constructs resulting from the assembly of organic molecules in the solid state is a central aim of crystal engineering. It is anticipated that precise control over solid state assembly processes will facilitate the synthesis of complex functional materials imbued with desirable optical, electronic, magnetic, and/or physical properties starting from carefully chosen yet relatively simple molecular precursors.[1] In turn, organic materials assembled in this manner may exhibit distinct advantages over their inorganic counterparts in terms of *inter alia* performance, miniaturization, and mechanical flexibility.

In particular, the design of organic semiconductors is an area of research that may benefit greatly from the development of successful crystal engineering synthetic strategies. The magnitude and efficiency of charge transport in solid state materials (crystals, films, polymers) composed of single-component redox-active organic compounds or multicomponent combinations of electron donor/acceptor organic compounds have been shown to critically depend on the relative orientation of molecular constituents. For example, numerous theoretical and empirical studies involving the prototypical organic conductor tetrathiafulvalene (TTF) and TTF derivatives indicate that charge mobility is enhanced when TTF components assemble in face-to-face intermolecular orientations.[2] Likewise, the presence of extended cofacial arene−arene contacts in polyacenes (a second family of organic conductors which includes tetracenes, pentacenes, perylenes, etc.) also leads to greater conductivity.[3] Consequently, several studies have described efforts aimed at directing (controlling) solid state assembly processes of TTFs, polyacenes, and TTF-acene hybrids to optimize the electronic properties of bulk material.[4]

We are interested in utilizing tetraarylethylenes as starting materials in crystal engineering approaches to a range of functional materials. Tetraarylethylenes comprise a family of organic compounds that possess interesting opto-electronic molecular properties, such as low redox potentials and solid state photoluminescence.[5] Substituted tetraarylethylene frameworks can be conveniently prepared in only a few synthetic operations so that functional groups important in directing intermolecular interactions (e.g., H-bond donors or acceptors) can be easily incorporated. Coupled with the reasonably well-defined shape and geometry of the tetraphenylethylene core, these compounds are seemingly attractive solid state supramolecular building blocks. Toward this end, we have prepared an electron-rich tetraarylethylene derivative symmetrically functionalized with four acetic acid groups. We report here the successful crystallization of this tetraarylethylene derivative with several bis(pyridine) reagents to afford semiconducting organic materials. We also demonstrate that the charge transport properties of these crystals can be modulated as a function of the bis(pyridine) component.

The compounds used in this study are illustrated in Figure 1. The tetracid **1** was easily prepared from the corresponding tetraphenol[6] via alkylation with ethyl bromoacetate followed by ester saponification. We initially envisioned that the carboxylic acid groups in **1** would each serve as H-bond donors along vectors approximating the sp^2 geometry of the central alkene carbons (despite the flexibility of the OCH_2 linkers connecting the acid groups to the tetraphenylethylene core). We reasoned that combining the tetratopic H-bond donor **1** with linear ditopic H-bond acceptors, such as bis(pyridine)s **BPE**, **BPEt**, or **Bpy**, may afford 2D sheet structures with alternating rows of tetraphenylethylene and bis(pyridine) components. Stacking of these 2D sheets might then result in potentially electroactive crystalline architectures featuring segregated columns of electron-rich and -deficient components (i.e., **1** and bis(pyridine), respectively).

Received: April 1, 2011
Published: April 27, 2011

dx.doi.org/10.1021/ja203001z | *J. Am. Chem. Soc.* 2011, 133, 8490–8493

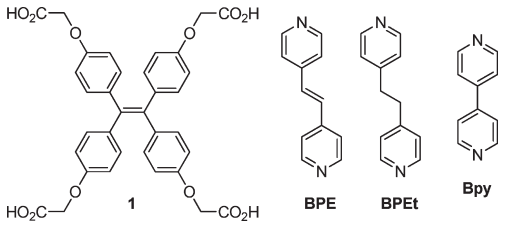

Figure 1. Crystallization components used in this study.

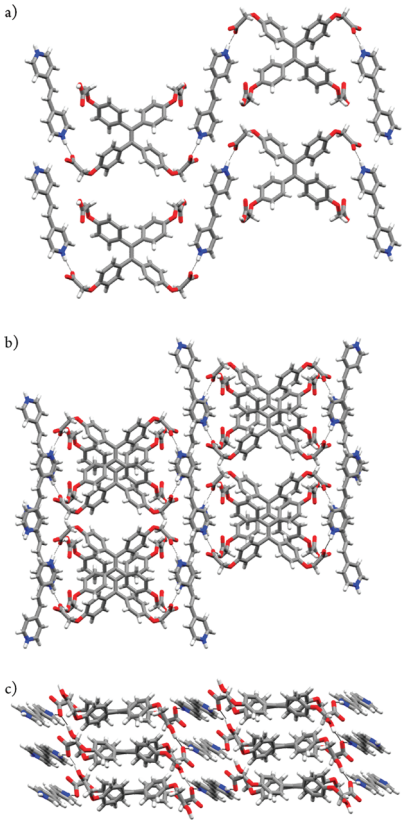

Figure 2. (a) 2D layer formed by charge-assisted H-bonding between **1** and **BPE** viewed down *c* (H-bonds shown as black lines). (b) Stacking of 2D layers (down *c*) mediated by $CO_2H\cdots{}^{-}O_2C$ H-bonding. (c) View of the crystal down *b* illustrating the segregated columns of **1** and **BPE**. Disordered solvate molecules omitted for clarity. Crystals of **1·BPEt** are isostructural with **1·BPE**.

Combining **1** with 2 molar equiv of **BPE**, **BPEt**, or **Bpy** in a mixture of acetone and methanol resulted in the deposition of single crystals upon slow solvent evaporation. Contrary to expectations, however, crystals of 1:1 stoichiometry were obtained in each case as determined by single crystal X-ray diffractometry. The structure of **1·BPE** illustrates many features common to all three structures. Molecules of **1** adopt propeller-like conformations typical of tetraphenylethylenes in the solid state.[7] Two carboxylic acid residues of **1** are engaged in charge-assisted H-bonding with pyridine nitrogen atoms. From the position of the hydrogen atoms and the similar C−O bond lengths in the relevant carboxylic acid residues, we conclude that transfer of a proton to the pyridine has occurred so that the H-bonding interaction can be described as involving a pyridinium H-bond donor and a carboxylate H-bond acceptor (N···O distance = 2.59 Å). Each molecule of BPE bridges two adjacent molecules of **1** (as we originally envisaged) to generate 2D layers (Figure 2a). Disordered solvent molecules (not shown) occupy the voids between adjacent molecules of **1**.

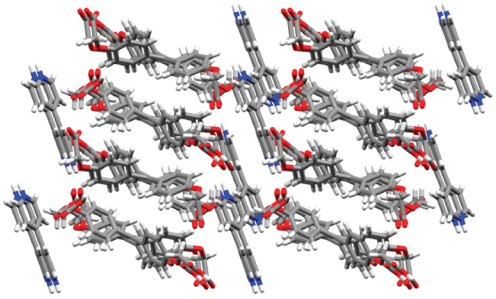

Figure 3. View of **1·Bpy** slightly offset from the *b* axis illustrating columns of **1** flanked by layers of **Bpy**. Disordered solvate molecules omitted for clarity.

The remaining carboxylic acid residues in **1·BPE** are involved in mediating the stacking of 2D layers through H-bonding interactions with carboxylate groups in adjacent layers. Two views of the extended packing are shown in Figure 2b,c. As a consequence of these stacking interactions, individual 2D layers are aligned 180° in a slightly offset fashion down the *c* axis to produce an *abab*-type pattern. This results in well-defined segregated columns of **1** and **BPE** (Figure 2c).

The single crystal structure of **1·BPEt** was found to be isostructural with **1·BPE**. Charge-assisted H-bonding between formally anionic carboxylate groups on **1** and dicationic bis(pyridinium)ethane units results in 2D layers analogous to that shown in Figure 2a. Layers are then stacked as shown in Figure 2b, c via additional $CO_2H\cdots{}^{-}O_2C$ hydrogen bonds (see Supporting Information (SI)). The only difference between the two structures is the presence of a π bond linking the two pyridinium groups in **BPE**, a structural feature that appears to exert a significant influence over the conductivity of the material (*vide infra*).

The structure of **1·Bpy** also features bis(pyridine) units bridging molecules of **1** via charge-assisted H-bonding. In this case, however, the crystal participants are arranged in a step-like fashion rather than distinct layers. Nonetheless, segregated columns of **1** are clearly evident (Figure 3). These columns are separated by layers of **Bpy** molecules oriented with their long axis roughly parallel with the direction of tetraarylethylene stacks.

The color of these crystals varied from pink to orange to pale yellow as the bis(pyridine) component changed from **BPE** to **Bpy** to **BPEt**. Coloration may indicate varying levels of charge-transfer interaction in the solid state, presumably facilitated by the electron-donating ability of **1** and the electron-accepting abilities of the bis(pyridine)s (which are expected to be enhanced by their conversion to bis(pyridinium) species in the crystals). Structural evidence for charge-transfer interactions, however, was not apparent from X-ray data. For example, elongation of the central alkene C=C bond in **1** (as might be expected if **1** acquires partial radical cation character) was not observed. This bond length ranged between 1.358 and 1.363 Å in the crystals examined, and these values are similar to the bond length reported for tetraanisylethylene (1.359 Å) and significantly shorter than the bond length reported for the tetraanisylethylene radical cation (1.417 Å).[7] Consequently, the electronic structure of these crystals was explored using quantum chemical calculations.

dx.doi.org/10.1021/ja203001z |*J. Am. Chem. Soc.* 2011, 133, 8490–8493

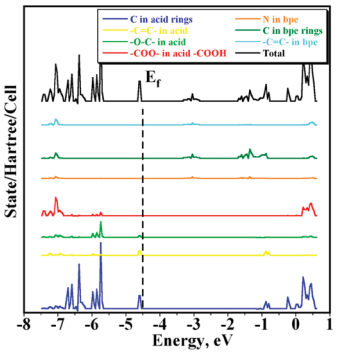

Figure 4. DOS calculation for **1·BPE**. Fermi energy (E_f, dashed line) corresponds to the energy of the HOCO.

Table 1. Physical and Electrical Properties of 1·Bis(pyridine) Crystals

crystal	color	Band gap[a] (eV)	ρ ($\Omega\cdot$cm)	σ ($S\cdot cm^{-1}$)	μ_{eff} ($cm^2/V\cdot s$)[c]
1·BPE	pink	1.28	3.6 ± 0.9	0.28 ± 0.06	0.38 ± 0.05
1·Bpy	orange	1.99	213 ± 70	$(4.7 \pm 1.3) \times 10^{-3}$	$(1.7 \pm 0.4) \times 10^{-2}$
1·BPEt	yellow	2.47	$>2.4 \times 10^6$	nc[b]	nc[b]

[a] Determined computationally from TDOS calculations. [b] Not calculated. [c] $\mu = \sigma^{0.76}$; see ref 10.

Experimentally obtained X-ray data were subjected to quantum chemical analysis in the form of atomic position optimization followed by density of states (DOS) calculations to identify the crystalline orbitals involved in charge-transfer processes.[8] Atomic projections of densities of states for **1·BPE** are shown in Figure 4 as the sum of contributions from (1) all carbon atoms, (2) C═C bonds, (3) O−C bonds, and (4) CO_2 functional groups in **1**; (5) nitrogen and (6) carbon atoms in **BPE**; and (7) C═C in **BPE** (bottom to top in Figure 4). The carbocycles in **1** emerged as the major contributors to the highest occupied crystalline orbital (HOCO) located at ~ −4.5 eV. The pyridyl carbon atoms and the C═C in **BPE** are calculated to be the dominant contributors to the lowest unoccupied crystalline orbital (LUCO) located at ~ −3.5 eV in Figure 4. The relatively small band gap found in **1·BPE** (1.28 eV) provides a basis for the apparent charge-transfer interactions. Similar computational treatment of **1·BPEt** and **1·Bpy** yielded HOCO levels of comparable energy (−4.5 eV). The LUCO levels, however, were shifted to slightly higher energies resulting in increased band gap values of 2.47 and 1.99 eV, respectively (see Table 1 and SI).

The electrical properties of these crystalline assemblies were then measured using conducting probe atomic force microscopy (CP-AFM). Bulk microcrystalline samples were prepared in good yield by concentration of equimolar solutions of **1** and **BPE**, **BPEt**, and **Bpy**. Samples prepared in this way were found to be homogeneous and possessed forms identical to those found in single crystals as determined by PXRD. All three microcrystalline samples were also found to be thermally stable up to ~175 °C as determined by TGA.

For the CP-AFM studies, each sample was deposited on a thermally evaporated Au substrate and imaged to determine the crystal morphology and shape. A typical crystal image for **1·BPE** is shown in Figure 5a. Crystals prepared from **BPEt** and **Bpy** were similar in appearance. Electrical measurements were

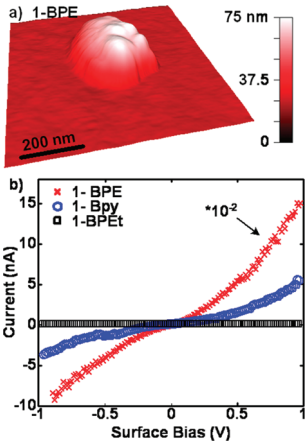

Figure 5. (a) Representative 3D crystal image for **1·BPE**. (b) Representative $I-V$ curves for **1·BPE** (red crosses), **1·Bpy** (blue circles), and **1·BPEt** (black squares). The **1·BPE** curve is scaled downward by a factor of 100 to fit on the indicated axes.

performed on individual crystals in an insulating organic solvent (bicyclohexyl) to prevent water layer contamination. Each measurement consisted of recording a series of repeated current−voltage ($I-V$) curves under 50 nN of force, which provided sufficient contact between the crystal and the tip without damaging the crystal. Each crystal was subjected to 15 $I-V$ measurements, and then the crystal was reimaged for comparison to the original image. Crystals exhibiting significant differences in images collected before and after conductivity measurements were not used in data analysis. Representative $I-V$ curves are shown in Figure 5b for **1·BPE**, **1·Bpy**, and **1·BPEt**. Note that the $I-V$ curve for **1·BPE** has been divided by a factor of 100 to be displayed on the same scale as the curves for the other two samples. From the representative data shown in Figure 5b it is clear that crystals of **1·BPE** are highly conductive, while **1·Bpy** is moderately conductive and **1·BPEt** shows no measurable current throughout the voltage bias range of the measurement.

The resistivity (ρ) of **BPE** and **Bpy** crystals was calculated using the linear region of the $I-V$ curves (bias range of ±0.15 V). This bias range was fit to Ohm's Law to obtain the resistance, and this value and values for crystal height (measured directly from AFM images) and probe-sample contact area (calculated to be 1850 ± 50 nm^2 using the Hertzian elastic model) were used to determine resistivity (see SI for details). These data, along with related conductivity values (σ), are shown in Table 1. The resistivity for **1·BPEt** crystals could not be determined due to the absence of measurable current within the detection limit of the instrument (10 pA). Thus, the resistivity value shown in Table 1 (2.4×10^6 $\Omega\cdot$cm) represents a lower limit.

Finally, we attempted to calculate effective charge mobilities (μ) for the two semiconducting crystalline samples using the space-charge limited current model.[9] This approach was not suited to these samples, however, as the data in both cases exhibited a nonlinear I vs V^2 relationship. Thus, charge mobilities were estimated using a simple empirical model advanced by Brown that relates charge mobility to conductivity ($\mu = \sigma^{0.76}$) as shown in Table 1.[10]

The data obtained from CP-AFM conductivity studies clearly show that **1·BPE** and **1·Bpy** function as crystalline organic semiconductors. Indeed, the estimated μ_{eff} for **1·BPE** (0.38 $cm^2/V\cdot s$) is comparable to charge mobilities determined for single crystals and crystalline films of well-established polyacene and

dx.doi.org/10.1021/ja203001z | J. Am. Chem. Soc. 2011, 133, 8490–8493

thiophene-based organic semiconductors.[4,11] Moreover, the results also demonstrate an ability to tune the semiconducting properties of these tetraarylethylene crystals as a function of the bis(pyridine) agent. The most conjugated bis(pyridine) reagent (**BPE**) afforded crystals with **1** exhibiting a conductivity approximately 2 orders of magnitude greater than that for crystals obtained from 4,4′-bipyridine, while crystals derived from **1** and nonconjugated **BPEt** were comparatively nonconducting. These conducting properties correlate nicely with the calculated DOS which revealed a systematic lowering of the lowest unoccupied conduction orbital (LUCO) energy in the series **1**·**BPEt**, **1**·**Bpy**, and **1**·**BPE** (compare Figures 4, S16, and S17). Coupled with the nearly identical HOCO energies across the series, the net effect of LUCO lowering was a narrowing of the crystal band gap energy.

Currently the relative contributions of **1** and the bis(pyridine) moieties in governing charge mobility are not known. The high conductivity exhibited by **1**·**BPE** and the absence of conductivity in **1**·**BPEt** despite their isostructural crystalline networks seemingly suggests a crucial role for the bis(pyridine) units as principal charge carriers. In the case of **1**·**BPE**, the combination of protonated **BPE** molecules arranged in roughly cofacial orientations and π-conjugation between facially stacked rings may facilitate charge transport in two dimensions (see Figures 2b, S1, and S2). In line with this conjecture, the diminished conjugation in **1**·**Bpy** may contribute to the attenuated conductivity in this sample while the absence of conjugation in **BPEt** renders this crystal an insulator.[12] This model relegates **1** to the role of a crystalline scaffold that properly orients and activates (through protonation/H-bonding) the pyridine components for charge transport. In this regard, other relatively simple polycarboxylic acids may fulfill a similar function and studies exploring this possibility are underway. Alternatively, **1** may also contribute in some degree to the conducting properties of these assemblies as a consequence of intermolecular arene edge-to-face interactions and/or participation in extended H-bonded networks.[13] The synthetic accessibility of additional tetraarylethylene and bis(pyridine) derivatives should facilitate formulation of systematic structure−activity studies designed to shed light on this issue.

In conclusion, we have successfully prepared and characterized a series of stable crystalline composites from acetic acid substituted tetraphenylethylene and three bis(pyridine)s. Two of these supramolecular assemblies were found to exhibit electrical conductivities comparable to those of established organic semiconductors as determined through CP-AFM. Importantly, the conducting properties of these crystals can be modulated as a function of a bis(pyridine) partner, opening exciting opportunities for construction of new tunable electroactive organic materials. This study also illustrates the potential of tetraarylethylenes to serve as attractive supramolecular building blocks.

■ ASSOCIATED CONTENT

Supporting Information. Synthesis and characterization details of **1** and **1**·bis(pyridine) crystals, crystallographic data, additional structural details, description of computational methods, details of CP-AFM measurements and conductivity calculations, PXRD, TGA, CIF files. This information is available free of charge via the Internet at http://pubs.acs.org.

■ AUTHOR INFORMATION

Corresponding Author
chris-pigge@uiowa.edu

■ ACKNOWLEDGMENT

We thank the Department of Chemistry, University of Iowa. F. C.P. thanks the College of Liberal Arts & Sciences and the Obermann Center for Advanced Studies for sponsorship of a Career Development Award.

■ REFERENCES

(1) (a) Desiraju, G. R. *Crystal Engineering − The Design of Organic Solids*; Elsevier: Amsterdam, 1989. (b) *Frontiers in Crystal Engineering*; Tiekink, E. R. T., Vittal, J., Eds.; John Wiley & Sons: Chichester, 2006. (c) Pigge, F. C. *CrystEngComm* **2011**, *13*, 1733–1748.

(2) (a) Fourmigué, M.; Batail, P. *Chem. Rev.* **2004**, *104*, 5379–5418. (b) Bryce, M. R. *J. Mater. Chem.* **1995**, *5*, 1481–1496.

(3) (a) Anthony, J. E. *Angew. Chem., Int. Ed.* **2008**, *47*, 452–483. (b) Anthony, J. E. *Chem. Rev.* **2006**, *106*, 5028–5048.

(4) (a) Murata, T.; Morita, Y.; Fukui, K.; Sato, K.; Shiomi, D.; Takui, T.; Maesato, M.; Yamochi, H.; Saito, G.; Nakasuji, K. *Angew. Chem., Int. Ed.* **2004**, *43*, 6343–6346. (b) Murata, T.; Morita, Y.; Yakiyama, Y.; Fukui, K.; Yamochi, H.; Saito, G.; Nakasuji, K. *J. Am. Chem. Soc.* **2007**, *129*, 10837–10846. (c) Baudron, S. A.; Avarani, N.; Batail, P.; Coulon, C.; Clérac, R.; Canadell, E.; Auban-Senzier, P. *J. Am. Chem. Soc.* **2003**, *125*, 11583–11590. (d) Payne, M. M.; Parkin, S. R.; Anthony, J. E.; Kuo, C.-C.; Jackson, T. N. *J. Am. Chem. Soc.* **2005**, *127*, 4986–4987. (e) Moon, H.; Zeis, R.; Borkent, E.-J.; Besnard, C.; Lovinger, A. J.; Siegrist, T.; Kloc, C.; Bao, Z. *J. Am. Chem. Soc.* **2004**, *126*, 15322–15323. (f) Gsänger, M.; Oh, J. H.; Könemann, M.; Höffken, H. W.; Krause, A.-M.; Bao, Z.; Würthner, F. *Angew. Chem., Int. Ed.* **2010**, *49*, 740–743. (g) Sokolov, A. N.; Friščić, T.; MacGillivray, L. N. *J. Am. Chem. Soc.* **2006**, *128*, 2806–2807. (h) López, J. L.; Atienza, C.; Seitz, W.; Guldi, D. M.; Martín, N. *Angew. Chem., Int. Ed.* **2010**, *49*, 9876–9880.

(5) (a) Hong, Y.; Lam, J. W. Y.; Tang, B. Z. *Chem. Commun.* **2009**, 4332–4353. (b) Mori, T.; Inoue, Y. *J. Phys. Chem. A* **2005**, *109*, 2728–2740. (c) Banerjee, M.; Emond, S. J.; Lindeman, S. V.; Rathore, R. *J. Org. Chem.* **2007**, *72*, 8054–8061. (d) Schreivogel, A.; Maurer, J.; Winter, R.; Baro, A.; Laschat, S. *Eur. J. Org. Chem.* **2006**, 3395–3404. (e) Hünig, S.; Kemmer, M.; Wenner, H.; Barbosa, F.; Gescheidt, G.; Perepichka, I. F.; Bäuerle, P.; Emge, A.; Peters, K. *Chem.—Eur. J.* **2000**, *6*, 2618–2632. (f) Wolf, M. O.; Fox, H. H.; Fox, M. A. *J. Org. Chem.* **1996**, *61*, 287–294.

(6) Schultz, A.; Diele, S.; Laschat, S.; Nimtz, M. *Adv. Funct. Mater.* **2001**, *11*, 441–446.

(7) Rathore, R.; Lindeman, S. V.; Kumar, A. S.; Kochi, J. K. *J. Am. Chem. Soc.* **1998**, *120*, 6931–6939.

(8) Dovesi, R.; Saunders, V. R.; Roetti, R.; Orlando, R.; Zicovich-Wilson, C. M.; Pascale, F.; Civalleri, B.; Doll, K.; Harrison, N. M.; Bush, I. J.; D'Arco, P.; Llunell, M. *CRYSTAL'09*; University of Torino: Torino, Italy, 2009.

(9) (a) Kao, K. C.; Hwang, W. *Electrical Transport in Solids*; Pergamon: Oxford, 1981; Chapter 3. (b) Coropceanu, V.; Cornil, J.; da Silva Filho, D. A.; Olivier, Y.; Silbey, R.; Brédas, J.-L. *Chem. Rev.* **2007**, *107*, 926–952.

(10) (a) Brown, A. R.; de Leeuw, D. M.; Havinga, E. E.; Pomp, A. *Synth. Met.* **1994**, *68*, 65–70. (b) Paasch, G.; Lindner, T.; Scheinert, S. *Synth. Met.* **2002**, *132*, 97–104.

(11) Molinari, A. S.; Alves, H.; Chen, Z.; Facchetti, A.; Morpurgo, A. F. *J. Am. Chem. Soc.* **2009**, *131*, 2462–2463 and references cited.

(12) We expect the magnitude of conductivity to also depend on the orientation of the crystal with respect to the AFM surface and tip. Measurements in this study were performed on randomly oriented crystals, and so mobility values likely represent an average from multiple crystal orientations.

(13) (a) Miao, Q.; Chi, X.; Xiao, S.; Zeis, R.; Lefenfeld, M.; Siegrist, T.; Steigerwald, M. L.; Nuckolls, C. *J. Am. Chem. Soc.* **2006**, *128*, 1340–1345. (b) Morita, Y.; Murata, T.; Fukui, K.; Yamada, S.; Sato, K.; Shiomi, D.; Takui, T.; Kitagawa, H.; Yamochi, H.; Saito, G.; Nakasuji, K. *J. Org. Chem.* **2005**, *70*, 2739–2744.